Heliyon 10 (2024) e33663

Contents lists available at ScienceDirect

Heliyon

journal homepage: www.cell.com/heliyon

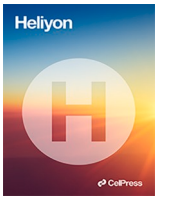

Research article

FYN-mediated phosphorylation of BCKDK at Y151 promotes GBM proliferation by increasing the oncogenic metabolite N-acetyl-L-alanine

Ling Zou [d,b,1], Wei Wang [b,1], Wenda Huang [e,b], Xiaofang Ni [b], Wensheng Li [b], Yue Cheng [b], Qin Tian [b], Lin Liu [b], Feng Zhu [a,c,**], Qiuhong Duan [a,b,c,*]

[a] Translational Medicine Center, Huaihe Hospital of Henan University, Kaifeng, Henan, 475000, China
[b] Department of Biochemistry and Molecular Biology, School of Basic Medicine, Tongji Medical College, Huazhong University of Science and Technology, Wuhan, Hubei, China
[c] The Zhongzhou Laboratory for Integrative Biology, Zhengzhou, Henan, 450000, China
[d] College of Biomedicine and Health and College of Life Science and Technology, Huazhong Agricultural University, Wuhan, Hubei, China
[e] Department of Neurosurgery, Tongji Hospital, Tongji Medical College, Huazhong University of Science and Technology, China

ARTICLE INFO

Keywords:
BCKDK
Fyn
Glioblastoma
N-acetyl-L-alanine
ACY1

ABSTRACT

Branched chain α-keto acid dehydrogenase kinase (BCKDK) is a key enzyme involved in the metabolism of branched-chain amino acids (BCAAs). Its potential as a therapeutic target and prognostic factor for a variety of cancers has been widely reported. In this study, we investigated the expression of BCKDK in clinical glioma samples and found that BCKDK was significantly overexpressed in glioblastoma (GBM) and was associated with its poor prognosis. We further found that BCKDK is phosphorylated by tyrosine protein kinase Fyn at Y151, which increases its catalytic activity and stability, and demonstrate through *in vivo* and *in vitro* experiments that BCKDK phosphorylation promotes GBM cell proliferation. In addition, we found that the levels of the metabolite N-acetyl-L-alanine (NAAL) in GBM cells with high BCKDK were higher than those in the silencing group, and silencing or inhibition of BCKDK promotes the expression of ACY1, an enzyme that catalyzes the hydrolysis of NAAL into acetic acid and alanine. Exogenous addition of NAAL can activate the ERK signaling pathway and promote the proliferation of GBM cells. Taken together, we identified a novel mechanism of BCKDK activation and found NAAL is a novel oncogenic metabolite. Our study confirms the importance of the Fyn-BCKDK-ACY1-NAAL signalling axis in the development of GBM and suggests that *p*-BCKDK (Y151) and NAAL can serve as potential predictors of GBM progression and prognosis.

* Corresponding author. Translational Medicine Center, Huaihe Hospital of Henan University, Kaifeng, Henan, 475000, China.
** Corresponding author. Translational Medicine Center, Huaihe Hospital of Henan University, Kaifeng, Henan, 475000, China.
E-mail addresses: 1092130572@qq.com (L. Zou), 489622753@qq.com (W. Wang), 1996@163.com (W. Huang), 2870415877@qq.com (X. Ni), 2628220830@qq.com (W. Li), 969127768@qq.com (Y. Cheng), cherry_tian9@yeah.net (Q. Tian), liulin2016@hust.edu.cn (L. Liu), fengzhu@hust.edu.cn (F. Zhu), duanqhwz@hust.edu.cn (Q. Duan).
[1] These authors contributed equally.

https://doi.org/10.1016/j.heliyon.2024.e33663
Received 10 October 2023; Received in revised form 20 June 2024; Accepted 25 June 2024
Available online 1 July 2024

1. Introduction

Glioblastoma (GBM) is a highly aggressive primary tumor that occurs in the central nervous system (CNS) and has a poor prognosis [1,2]. The median overall survival (mOS) for patients with GBM is typically only 12–18 months, and the 5-year survival rate is as low as 5 % [3–6]. Despite the identification of various molecular subtypes and altered signaling pathways in GBM, the number of drugs approved by the Food and Drug Administration (FDA) for GBM treatment is limited. It is crucial to fully comprehend the mechanisms underlying the development of GBM in order to discover more effective treatment options.

Metabolic reprogramming is one of the hallmark features of tumor cells [7,8]. Tumor cells can be promoted to proliferate during their development by adjusting or changing the levels of metabolites, which are called oncometabolite [28]. The altered metabolism of branched chain amino acid (BCAAs), including valine, leucine and isoleucine, have been revealed to associate with tumorigenesis and progression [9–12]. Branched chain amino acid transaminase (BCAT) catalyzes the deamination of BCAA to produce branch chain α-keto acids (BCKAs) [13–15]. BCKAs is used for energy by branched chain α-keto acid dehydrogenase complex (BCKDC)-catalyzed irreversible oxidative decarboxylation in mitochondria. BCKD kinase (BCKDK) could inhibit BCKDC activity by phosphorylating its alpha subunit, branched chain α-keto acid dehydrogenase (BCKDHA) at S293 site to suppress the catabolism of BCAAs [16,17]. Therefore, regulation of BCKDK activity constitutes a major mechanism for BCAAs homeostasis *in vivo*. Recently, East, M. P. believed that BCKDK is an emerging kinase target for tumors [18]. Our previous research has also revealed that BCKDK activation by Src can promote tumorigenesis and metastasis of colorectal cancer [19,20], and BCKDK could phosphorylate BCAT1 to promote the progression of GBM [21]. In addition, studies in breast [22,23] and lung cancer [24] have confirmed that BCKDK may be a therapeutic target for cancer and enhance the accumulation of BCAAs and BCKA in disease states. However, BCKDK is one of 162 "dark kinases" whose function in human biology is poorly understood [25] (https://darkkinome.org/). The mechanism of BCKDK activation and its effector remain poorly understood, especially in tumorigenesis and progression.

To date, only six downstream substrates and two upstream kinases of BCKDK have been reported. In addition to BCKDHA, BCKDK could also phosphorylate ATP citrate lyase (ACL) which promoted fat synthesis in liver cells [26], pyruvate dehydrogenase complex (PDC) which regulated pyruvate metabolism [27] and MEK at S221 site to promote colorectal cancer tumorigenesis by activating the MEK-ERK cascade [19]. Recently, we found that BCKDK phosphorylated BCAT1 (S5, S9, and T312) and STIP1 homology and u-box protein 1 (STUB1) (S19) to promote glioma cell proliferation [21]. Src kinase is the first upstream kinase to be shown to directly phosphorylate and activate BCKDK at Y246 to promote metastasis of colon cancer [20]. In addition, APN also mediates the phosphorylation of BCKDK S31, which activates the ERK signalling pathway in HCC cells [28]. Although studies have shown that BCKDK can promote the growth of cancer cells by activating growth signaling pathways, and is also involved in the regulation of BCAAs, glucose and lipid metabolism, the activation mechanism, downstream effector and biological functions of BCKDK under certain diseases or specific signal stimuli need to be further studied.

In this study, we found that BCKDK exhibits high levels of expression in GBM and is activated by Fyn kinase at Y151. Additionally, we identified that the metabolite NAAL, which is regulated by BCKDK, can serve as a marker for GBM proliferation. These findings shed light on the molecular mechanism of the Fyn-BCKDK signaling axis in glioma development and suggest that *p*-BCKDK (Y151) and NAAL can serve as potential predictors of glioma progression and prognosis.

2. Material and methods

2.1. Cell culture and stable cell line generation

The H4, U87, U118, A172, Hs683, GL261 and HEK293T cell lines were purchased from American Type Culture Collection (ATCC; Manassas, VA, USA) and cultured with Dulbecco's modified Eagles' medium (Gibco, Grand Island, NY) containing 10 % fetal bovine serum (FBS; Gibco). All cells were cultured in a humidified environment at 37 °C with 5 % CO_2.

The sgRNA or shRNA of target Fyn and BCKDK, synthesized by Tsingke Biotechnology, were computationally identified (http://www.e-crisp.org/E-CRISP/designcrispr.html, https://rnaidesigner.thermofisher.com/rnaiexpress/sort.do, Table 1), cloned and inserted into the Lenti-Crispr V2/pLKO.1 vector to obtain the corresponding plasmid. The sgRNA or shRNA plasmids and lentiviral vectors (psPAX2 and pMD2. G) were mixed in the presence of SimpleFect (Signaling Dawn Biotechnology, Wuhan) and then transfected to produce lentiviral particles in HEK293T cells. Medium containing lentivirus was collected 48 h after transfection, filtered through a 0.22 μm filter and added to U87 and U118 cell cultures containing polyene (10 μg/ mL) and screened with puromycin (APExBio. Houston, USA) at least 3 d.

GL261-or U87-Luc cell line was obtained by transient transfection of pLVX-Luc-GFP and screening with G418 for at least 2 weeks. GL261-Luc-, H4- or A172-BCKDK stable cell lines were established by lentiviral packaging (as before) using pHAGE-Myc-BCKDK-Flag

Table 1
A list of regents and antibodies in this study.

sgRNA	Sequence
sgFyn#1	5′-CACCGGGGACCTTGCGTACGAGAGG-3′
sgFyn#2	5′-CACCGGGCTCCAGTTGACTCTATCC-3′
sgBCKDK#1	5′-CACCGTAGCGGATCCTCAGTCCTAG-3′
sgBCKDK#2	5′-CACCGGACTGTTCGAGCCCTTCCGC-3′

plasmid.

2.2. Western blot (WB) and immunoprecipitation (IP)

Cells were lysed in RIPA buffer, sonicated 3 times on ice and centrifuged at 4 °C for a further 15 min. The supernatant fractions were quantified using Bradford assay reagent (Bio-Rad Laboratories, Inc.). 40–60 μg separated using SDS-PAGE and transferred to a PVDF membrane. After blocking with 5 % non-fat milk or 5 % BSA for 30 min, the membranes incubated with specific primary antibodies overnight at 4 °C. Subsequently the membranes were incubated with HRP-conjugated secondary antibodies for 1 h at room temperature, and antibody-bound proteins were visualized using chemiluminescence (Bio-Rad, USA). Cells were lysed using ice-cold IP buffer and the cell lysates were collected and immunoprecipitated with the specified antibody. After washing three times in cold IP buffer, the immunocomplexes were collected and subjected to WB. Relevant reagents and antibodies are shown in Table 2.

2.3. Clinical specimens, tissue microarray and immunohistochemical (IHC) staining

The glioma tissue microarrays (HBraG177Su01) were purchased from Shanghai Outdo Biotech CO., Ltd. The tissue samples of 32 glioma patients were obtained from Neurosurgery, Tongji Hospital, Tongji Medical College, Huazhong University of Science and

Table 2
A list of target sequences for sgRNAs and shRNA.

Antibody	Catalog Number	Source
Anti-BCKDK (E-12)	sc-374425	Santa Cruz Technology (CA, USA)
Anti-Fyn	sc-434	
Anti-MEK1/2	#8727	Cell Signaling Technology (Danvers, MA, USA)
Anti-p-MEK1/2 (S221)	#2338	
Anti-His	#2365s	
Anti-HA-tag	#3724	
Anti-p-BCKDHA (S293)	ab200577	Abcam (Cambridge, UK)
Anti-BCKDHA	ab68094	
Anti-BCKDK	PA5-86367	Thermo Fisher (Waltham, MA, USA)
Anti-Alpha Tubulin	66031-1-Ig	Proteintech (Wuhan, China)
Anti-Myc-tag	16286-1-AP	
Anti-Myc-tag	60003-2-Ig	
Anti-GST-tag	66001-2-Ig	
Anti-ubiquitin	10201-2-AP	
Anti-ACY1	11316-1-AP	Proteintech (Wuhan, China)
Anti-p-Thr	AB1607	Sigma-Aldrich (St. Louis, MO, USA)
Anti-Ser	05-1000	
Anti-Flag	F7425	
Anti-Flag	F1804	
Anti-p-BCKDK (Y151)		Abiocode (Shanghai, China)
HRP-conjugated secondary antibodies (R)	E030120-2	EarthOx Life (San Francisco, CA, USA)
HRP-conjugated secondary antibodies (M)	E030110-02	

Regent	Catalog Number	Source
3,6-dichlorobenzothiophene-2-carboxylic acid (BT2)	ZC-26488	ZZBIO.CO.LTD (Shanghai, China)
γ-32P-ATP	BLU002H250UC	Perkin Elmer (Beijing, China)
inactive human BCKDK recombinant protein	(TP303601)	Beijing OriGene Technology
Fyn active kinase	#14-441	Millipore Corp (Billerica, MA, USA)
Cycloheximide (CHX)	C7698-5G	Sigma-Aldrich (St. Louis, MO, USA)
Polybrene	TR-1003-G	
Puromycin	B7587	APExBio (Houston, USA)
G418 was purchased from GLPBIO (Montclair, CA)	GC17427	GLPBIO (Montclair, CA)
N-acetyl-L-alanine	S20262	Shyuanye (Shanghai, China)
D-Luciferin sodium salt	S19261	
Isopropyl β-D-thiogalactoside (IPTG)	ST098	Beyotime (Shanghai, China)

Plasmid	Catalog Number	Source
pcFlag-Fyn-WT	#74509	addgene (Cambridge, MA, USA)
phage	#118692	
lentiCRISPR V2	#52961	
pCMV-BCKDK-Flag WT		Laboratory owned and self-constructed
pCMV-BCKDK-Flag Y151F		
pcDNA4-His-BCKDK		
pcDNA4-His-BCKDK Y151F		
phage-Myc-BCKDK-Flag WT		
phage-Myc-BCKDK-Flag Y151F		
phage-Myc-BCKDK-Flag Y151D		
pET23a-BCKDK-His		

Technology (HUST). This study was performed with the permission of the ethical committee of Tongji Medical College, HUST.

The IHC staining was performed using BCKDK antibodies with 1:200 dilution. The scores of IHC were according to the staining intensity and percentage of positive cells. The result was considered positive if the multiplication of two scores was >3.

2.4. In vitro growth curve analysis (MTT assay)

To assess cell growth, cells (6×10^3/well) were inoculated in 96-well plates and incubated for 24, 48 and 72 h. Brominated 3-(4,5-dimethylthiazol-2-yl)-2,5-diphenyltetrazolium (MTT) was added to each well, and the reaction was terminated by the addition of 150 μL of dimethylsulfoxide (DMSO) after incubation for 4 h. When the purple crystals were completely dissolved, the reaction was performed on enzyme immunoassay analyser (Bio-Rad) at 490 nm.

2.5. Anchorage-independent growth assay (soft agar assay)

A total of 8×10^3 cells/well were seeded in a 6-well plate and cultured in 1 mL 0.33 % Basal Medium Eagle (BME) agar containing 10 % FBS, maintained at 37 °C, 5 % CO_2 for 3–5 w. The medium was changed every 5 d and the colonies were observed under microscope.

2.6. Colony formation assay

To assess ability of colony formation, the cells (2×10^3 cells/well) were seeded in 6-well plates and cultured in 37 °C, 5 % CO_2 incubator for 2–4 w. The medium was changed every 5 d. After the cells grew to an appropriate density, the colonies were washed twice with PBS, fixed with 4 % paraformaldehyde for 30 min and stain with 0.1 % crystal violet for 30 min. The cells were washed once with PBS, and were taken pictures after drying.

2.7. Immunofluorescence (IF) staining

U118 cells were seeded on cover glass (sigma, USA) and then fixed in 4 % paraformaldehyde for 30 min, permeabilized in Triton-X100 for 30 min and incubated with 5 % FBS for 30 min at room temperature. Samples are then washed and incubated overnight at 4 °C in a wet box with primary antibody. On day 2, cells are washed and incubated with Alexa Fluor 488 (green for BCKDK) or Alexa Fluor 546 (red for Fyn) secondary antibodies for 1 h at room temperature in a wet box, and chromatin is stained with DAPI. Images were observed and collected under a fluorescent microscope.

2.8. Bacterial expression and in vitro pull-down assay

The bacteria with pET23a-BCKDK-His were grown at 37 °C to an absorbance of 1.3–1.4 at 600 nm. The bacteria were washed with PBS for 4 times and lysed by repeated freeze-thaw from −20 °C to 37 °C. Then the bacteria were sonicated 3 times on ice for 10 min and centrifuged at 12000 rpm for 20 min. The precipitate was lysed with 8 M urea, and the supernatant was collected after centrifugation at 12000 rpm. The supernatant is incubated with Ni-NTA agarose overnight at 4 °C to obtain purified BCKDK-His protein for *in vitro* pull-down assay. The purified protein incubated with the cell lysates, and then rotated overnight at 4 °C. After unbound proteins was removed by washing in cold IP buffer, the bound proteins were detected by WB with the specific antibody.

2.9. In vitro kinase assay

Active Fyn kinase and the inactive BCKDK protein or peptide (KDQADEAQY$_{151}$CQLVRQLL, ARRLCEHKY$_{246}$GNAPRVRI) were incubated in 1 × kinase buffer containing 1 μCi γ-^{32}P-ATP or 100 μM ATP at 37 °C for 2 h. Finally, the phosphorylation signal was detected by autoradiography (Amersham Typhoon IP. GE, USA) or by WB using the specific phospho-antibody.

2.10. Cycloheximide (CHX) chase-assay

The cells were starved for 12 h and treated with 80 ng/ mL EGF. Then 100 μg/ mL of CHX was added to the medium to block the new protein synthesis. Cells were harvested at a range of time points and the levels of proteins were analyzed by WB. Half-life ($t_{1/2}$) is calculated by GraphPad Prism 7.0 software.

2.11. Intracranial xenograft GBM mouse model

4-week-old SPF-grade C57BL/6 and BALB/c-nu female mice were purchased from Beijing Vital River Laboratory Animal Technology Co., Ltd. and raised in the SPF-grade Experimental Animal Center of Tongji Medical College, Huazhong University of Science and Technology. The experimental protocol complied with the Hubei Provincial Regulations on the Administration of Laboratory Animals and the Regulations of the Laboratory Animal Ethics Committee of HUST, and was approved by the Laboratory Animal Ethics Committee of Tongji Medical College of HUST. A total of 5 μL (1×10^5) glioma cells (GL261-Luc-BCKDK for C57BL/6 mice U87-Luc-sgBCKDK for BALB/c-nu mice) were injected into the right striatum of the brain to construct the orthotopic transplanted tumor models.

Insert the needle about 3.5 mm deep from the scalp and leave it on for about 2 min before slowly pulling it out. To observe the tumour growth, anaesthetized mice were intraperitoneally injected with 150 mg/kg D-fluorescein (Yuanye, Shanghai, China) on the 14th and 21st days after cell injection, respectively, and images of the tumour region were acquired by an *in vivo* imaging system (IVIS) after 3 min. Neurological symptoms (cranial protrusion, hunchback, extreme lethargy or weight loss) were observed at any time, and the OS time of the mice was recorded.

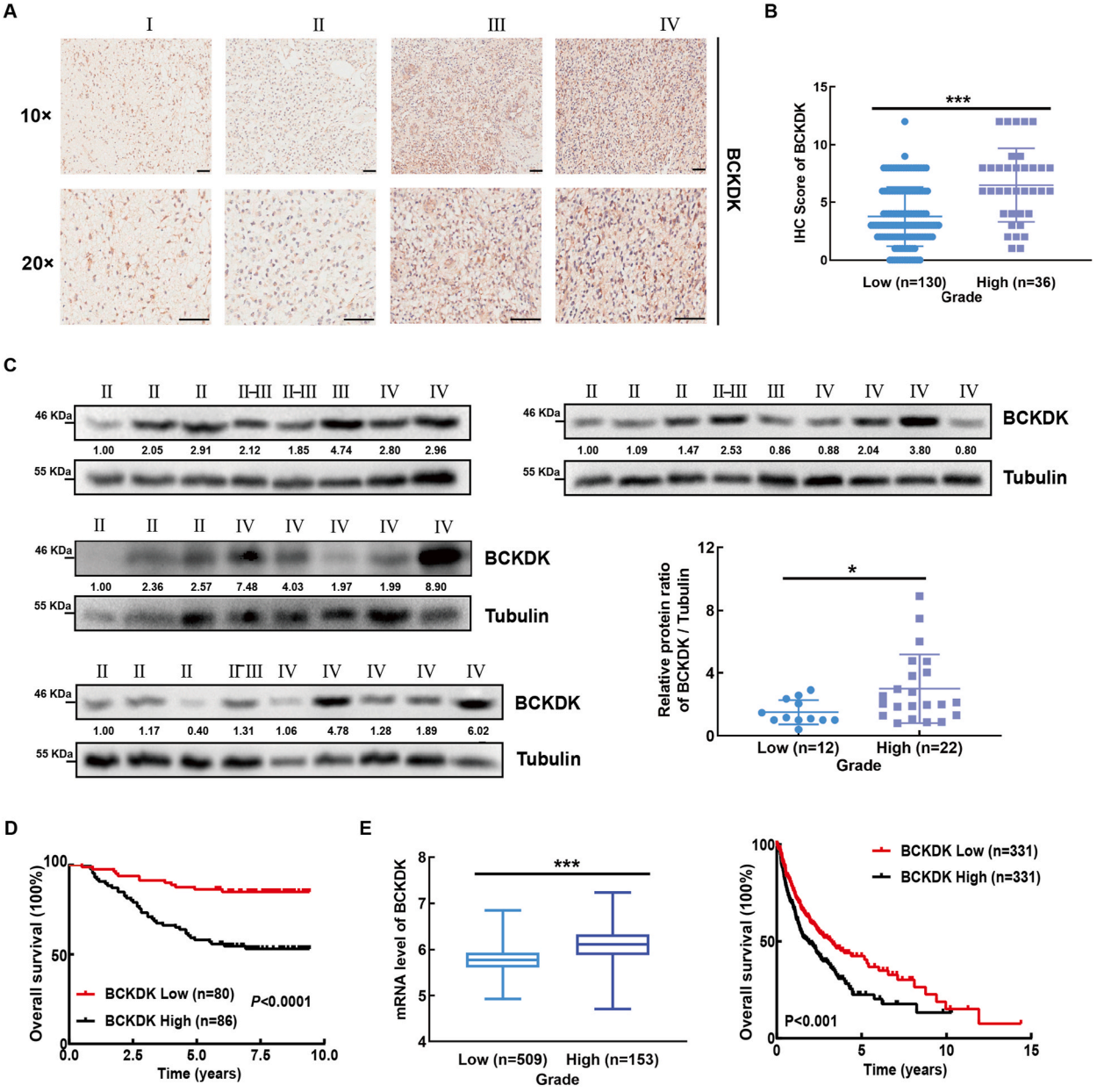

Fig. 1. BCKDK is highly expressed in GBM tissue and is positively correlated with poor prognosis of patients. A, Immunohistochemical (IHC) staining of BCKDK from 166 cases of glioma patients in the TMA. Representatives of IHC staining of BCKDK from different grades of glioma (upper panel) (10 × , 20 × , scale bar = 100 μm). B, The correlation between the protein level of BCKDK and the grades of glioma (down left panel). Kaplan-Meier analysis of OS. C, BCKDK protein level of 34 cases glioma patients were analyzed by WB. Statistical analysis on the correlation between protein level of BCKDK and grade (right down panel). The ratio values represent the levels normalized to BCKDK ratio Tubulin in each sample. D, The mRNA levels of BCKDK in different grades of glioma. E, Kaplan-Meier analysis of OS in glioma patients. The Data was obtained from TCGA database and analyzed by GraphPad Prism 7.0 software. *(*p < 0.05, ***p < 0.001)*.

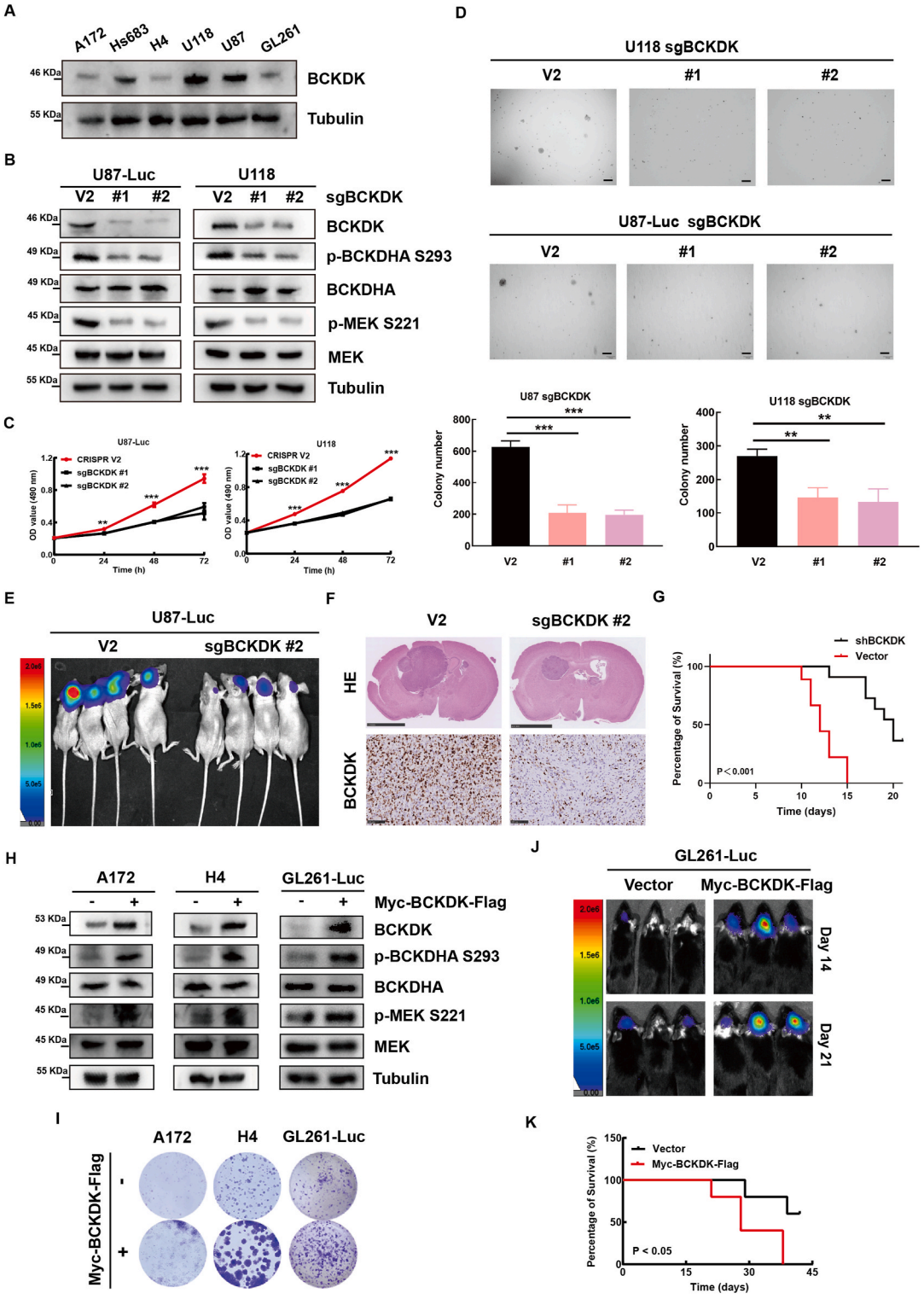

Fig. 2. BCKDK promotes GBM proliferation *ex vivo* and *in vivo*. A, the protein levels of BCKDK in 6 glioma cell lines were analyzed by WB. B, the effect of BCKDK knockdown on the expression of its downstream signaling molecules was examined by WB. The data are representative pictures of three replicates. C, Growth curve of BCKDK knockdown cell lines were determined by MTT assay. The data are presented as the mean ± SD of three replications. D, Soft agar of BCKDK knockdown cell lines. Scale bar: 200 μm. The data are presented as the mean ± SD of three replications. E, Tumor size by *in vivo* bioluminescence in xenograft tumor-bearing BALB/c-nu mice with silenced BCKDK cell lines. F, The intracranial tumor sections of control group and experimental group of nude mice were stained with HE. G, the OS curves of BALB/c-nu mice with GBM xenografts are

built according to the Kaplan-Meier methods. n = 8 *(***p < 0.001)*. H, the effect of stable overexpression of BCKDK on the expression of its downstream signaling molecules was examined by WB. The data are representative pictures of three replicates. I, Colony formation assay of control and BCKDK stable cells. J, Tumor size of BCKDK stable overexpression cell lines in xenograft mice was detected using bioluminescence on day 14 and day 21. K, the OS curves of C57 mice with GBM xenografts are built according to the Kaplan-Meier methods. n = 8 *(*p < 0.05)*.

2.12. Metabolomics

Metabolomic analyses of sgBCKDK cell lines were performed according to the protocal. Cells were washed 3 times with ice-cold PBS and rapidly frozen in liquid nitrogen. The cell metabolites were extracted with 1 mL pre-cooled extractants (80 % methanol aqueous solution) and analyzed by LC-ESI-MS/MS (MetWare, Wuhan, China). The identified metabolites were annotated using the KEGG Compound database, and then the annotated metabolites were mapped to the KEGG Pathway database.

2.13. NAAL quantitative analysis assay

Collect cell culture supernatants and cell lysates for NAAL concentration assays as described above. The collected serum samples were filtered at 0.22 μm for NAAL concentration detection. The samples and 1 μM NAAL standard as a control should be filtered by 25 mm × 0.22 μm filter before testing by Ultra Performance Liquid Chromatography (UPLC)/ESI-Q TRAP-MS/MS. The NAAL concentrations were standardized by protein concentration between groups.

2.14. Statistical analyses

The data in the study were expressed as means ± SD from at least three independent experiments. All dates were performed using GraphPad Prism 7.0 software (GraphPad, San Diego, CA). Student's *t*-test or one-way ANOVA were used to analyze two groups or multiple groups, respectively. $*p < 0.05$; $**p < 0\ 01$; $***p < 0.001$ was considered as significant.

3. Results

3.1. BCKDK is highly expressed in GBM tissue and positively correlated with poor prognosis of patients

In our previous studies, high expression of BCKDK was proved to promote tumorigenesis and metastasis of colorectal cancer [19,20]. In order to explore whether BCKDK can promote glioma progression, IHC staining was performed to detect the expression of BCKDK in 166 TMAs, and it was found that the expression of BCKDK was increased in high-grade glioma (Fig. 1A and B). Subsequently, we measured the protein level of BCKDK in 34 clinical glioma samples by WB, and found that the BCKDK level in high-grade gliomas was higher than those in low-grade (Fig. 1C). BCKDK protein levels were negatively correlated with the mOS of glioma patients (Fig. 1D). TCGA database analysis also showed that BCKDK mRNA levels were positively correlated with glioma grade and negatively correlated with the mOS of patients (Fig. 1E). These results suggested that high expression of BCKDK plays an important role in GBM.

3.2. BCKDK promotes GBM proliferation ex vivo and in vivo

It has been reported that elevated BCKDK could promote colorectal cancer tumorigenesis by upregulating the MEK-ERK signaling pathway [19]. To address the role and mechanism of BCKDK in the occurrence and development of GBM, we detected the endogenous expression of BCKDK in 6 glioma cell lines (Fig. 2A), and established BCKDK knockdown cell lines in U87-Luc or U118 cell lines by lentiviral infection (Fig. 2B). Next, the MTT and soft agar assay results indicated that the cell proliferation and clone-forming ability of BCKDK-silenced cells were weaker than control cells (Fig. 2C and D). Similar results were observed in BT2-treated U118 or Hs683 cells (Fig. S1A-C). These results indicated that knockdown or inhibition of BCKDK in glioma cells inhibited tumor growth *ex vivo*. Additionally, transplanted U87-Luc-sgBCKDK tumors grew significantly slower than those with V2 in the brains of BALB/c-nu mice and mice with U87-Luc-sgBCKDK had a better prognosis (Fig. 2E–G). Further, we established cell line stably expressing BCKDK in GL261-Luc, H4 and A172 cells (Fig. 2H). The results showed that the proliferation ability of cells expressing BCKDK increased by colony formation assays ((Fig. 2I), and transplanted GL261-Luc-BCKDK tumors grew significantly faster than those with vector in the brains of C57BL/6 mice and mice with GL261-Luc-BCKDK had shorter survival (Fig. 2J and K). Overall, BCKDK promotes GBM proliferation *in vitro* and *in vivo*.

3.3. Fyn directly binds with and phosphorylates BCKDK at Y151 site and enhances the activity of BCKDK

Our previous research found that the oncogene Src can phosphorylate BCKDK at Y246 and activate BCKDK in colon cancers [20]. Fyn, a member of the Src family, plays an important role in the occurrence and development of GBM [29–32]. Therefore, we speculated that Fyn may be an upstream kinase of BCKDK. First, we detected the levels of Fyn in 6 glioma cells and found that cells with high levels of BCKDK also expressed high Fyn (Fig. 2A and 3A), and that they co-localized in U118 cells (Fig. 3B). The results of IP assay and pull-down assay suggested that Fyn can bind with BCKDK (Fig. 3C and D). Subsequently, isotope kinase experiments showed that actived Fyn can phosphorylate BCKDK (Fig. 3E). To clarify the specific phosphorylation site of BCKDK by Fyn, we analyzed the protein

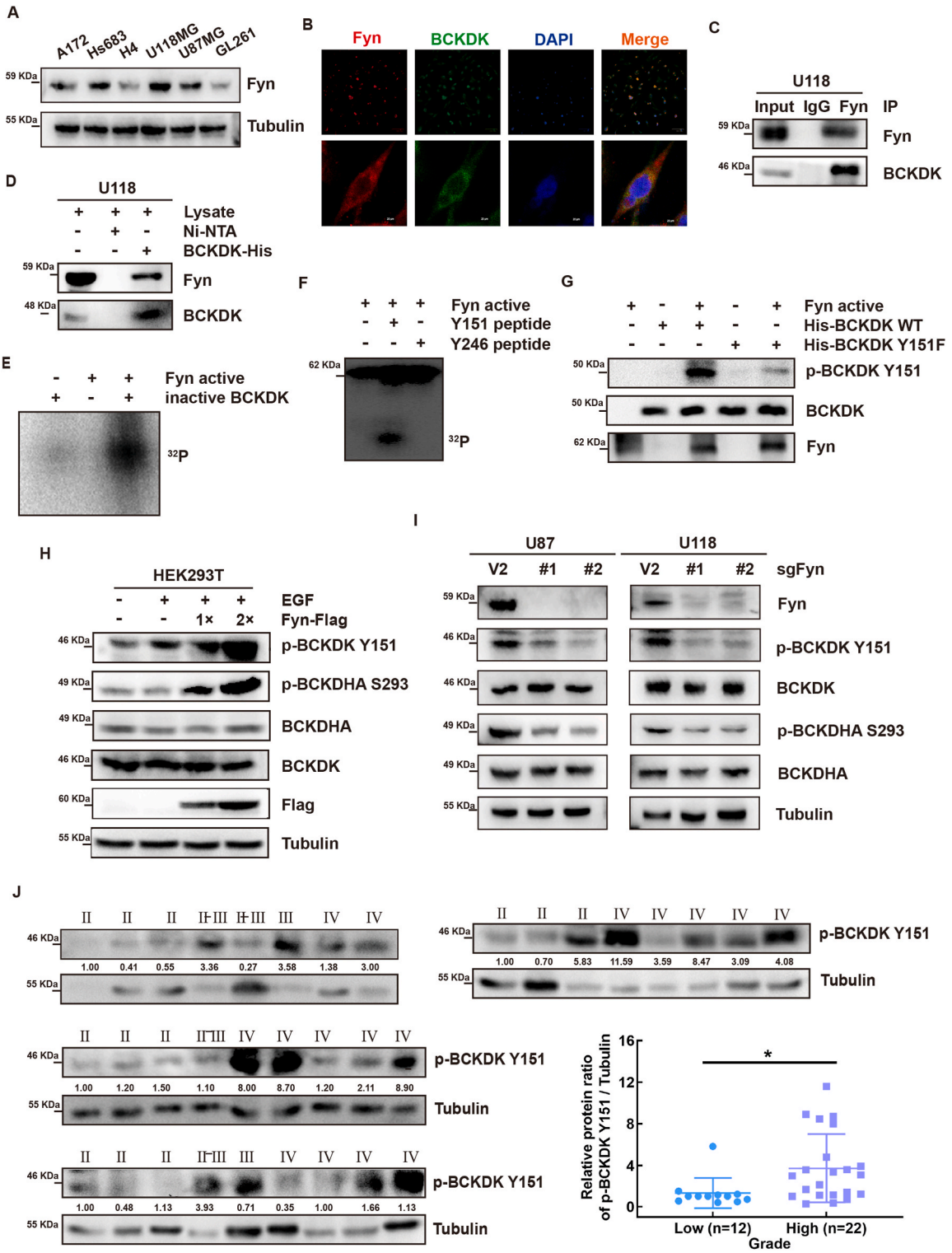

Fig. 3. Fyn binds with and phosphorylates BCKDK at Y151 site *in vitro* and enhances the activity of BCKDK *ex vivo*. A, the protein expression of Fyn in 6 glioma cell lines were analyzed by WB. B, Representative immunofluorescence for BCKDK (green) and Fyn (red) in U118 cells. Scale bar, 100 μm and 20 μm. C, *In vitro* pulldown assay was performed to detect Ni-NTA-His-BCKDK bound with endogenous Fyn in U118 cells. D, Endogenous BCKDK was co-immunoprecipitated with Fyn in U118 cells. E, Active Fyn phosphorylated inactive BCKDK *in vitro* in the presence of γ-^{32}P-ATP as visualized by autoradiography. F, Active Fyn phosphorylated BCKDK Y151 peptides *in vitro* in the presence of γ-^{32}P-ATP. G, BCKDK-WT protein and BCKDK-Y151F proteins as substrates for active Fyn *in vitro* were detected by WB using *p*-BCKDK (Y151) antibody. H, the phosphorylation and the activity of

BCKDK was detected by WB with the *p*-BCKDK Y151 and *p*-BCKDHA S293 antibody in HEK293T cells transfected with Fyn-Flag plasmids under EGF (80 ng/ mL, 15 min) stimulation. I, the phosphorylation and the activity of BCKDK was detected by WB in cell silencing Fyn. The data are representative pictures of three replicates. J, *p*-BCKDK Y151 protein level of glioma tissues were analyzed by WB. Statistical analysis on the correlation between protein level of *p*-BCKDK Y151 and grade (*$p < 0.05$). . (For interpretation of the references to color in this figure legend, the reader is referred to the Web version of this article.)

sequence of BCKDK with NetPhos 3.1 software, synthesized two highly scored BCKDK peptides (Y151 and Y246), and performed isotope kinase experiments. The results showed that active Fyn significantly phosphorylated the Y151 site of BCKDK, but not the Y246 site (Fig. 3F). To further confirm the phosphorylation BCKDK at Y151 site, we prepared phospho-antibodies recognizing phosphorylated BCKDK (Y151) and purified prokaryotic expression of BCKDK-Y151F protein for *in vitro* kinase assay. Fig. 3G result showed the phosphorylation level of BCKDK-Y151F significantly decreased. These results suggested that Fyn is a direct upstream kinase of BCKDK and phosphorylated it at the Y151.

To determine whether the BCKDK Y151 phosphorylation modification is also present in cells, we transfected the Fyn plasmid into

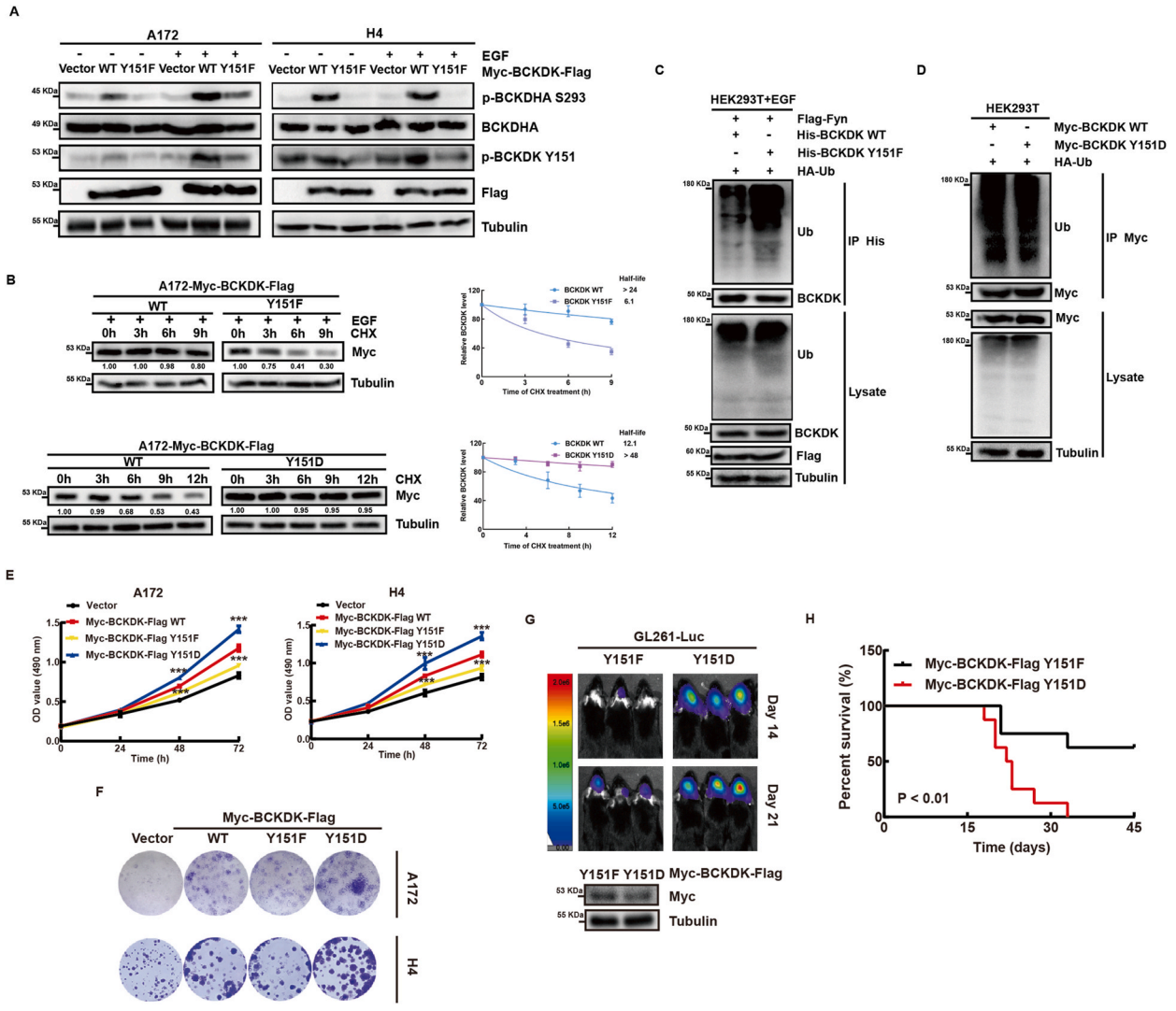

Fig. 4. Fyn phosphorylates BCKDK at the Y151 site to increase its activity and stability to promote glioma proliferation. A, WB of BCKDK-WT and BCKDK-Y151F stable A172 or H4 cells with or without EGF (80 ng/ mL) stimulation for 30 min. B, the levels of BCKDK were detected by WB in BCKDK-WT and BCKDK-Y151F stable A172 cells treated with CHX and EGF stimulation or in BCKDK-WT and BCKDK-Y151D stable A172 cells only treated with CHX. The data are presented as the mean ± SD of three replications. C and D, the ubiquitination of the BCKDK were analyzed by WB in HEK293T cells transfected with indicated plasmids. E, Growth curves of control and BCKDK stable cell lines by MTT assay. The data are presented as the mean ± SD of three replications. (*$p < 0.01$, **$p < 0.001$). F, Colony formation assay of control and BCKDK stable cells. G, Live images of C57 mice with luciferase-labeled GL261 cells expressing BCKDK-Y151F or BCKDK-Y151D xenografts on day 14 and day 21 are shown by bioluminescence. H, Kaplan-Meier survival curve of C57 mice. n = 8 (*$p < 0.01$).

HEK293T cells and observed the intracellular phosphorylation levels of BCKDK and BCKDHA by WB. The results showed that the levels of *p*-BCKDK and *p*-BCKDHA increased in Fyn dose-dependent manner in HEK293T cells (Fig. 3H). The levels of *p*-BCKDK and *p*-BCKDHA significantly reduced in U87- or U118- sgFyn cells (Fig. 3I). Moreover, we also found that the level of *p*-BCKDK were significantly higher in high-grade glioma tissues (grade 3 and 4) than in low-grade glioma tissues (Grade 1 and 2). by WB using a *p*-BCKDK (Y151) antibody (Fig. 3J). These results suggested that Fyn activates BCKDK as a direct upstream kinase by phosphorylation at Y151 and that the levels of *p*-BCKDK (Y151) correlates with glioma grade.

3.4. *Fyn phosphorylates BCKDK at the Y151 site to increase its activity and stability to promote glioma proliferation*

In order to clarify the biological effect of phosphorylation of BCKDK at Y151, we overexpressed BCKDK-WT, BCKDK-Y151F and BCKDK-Y151D in A172 and H4 cells. Fig. 4A shows that the *p*-BCKDHA levels in cells with BCKDK-Y151F are lower than those with BCKDK-WT, indicating reduced activity of BCKDK-Y151F. We also tested whether BCKDK phosphorylation at Y151 affects its stability.

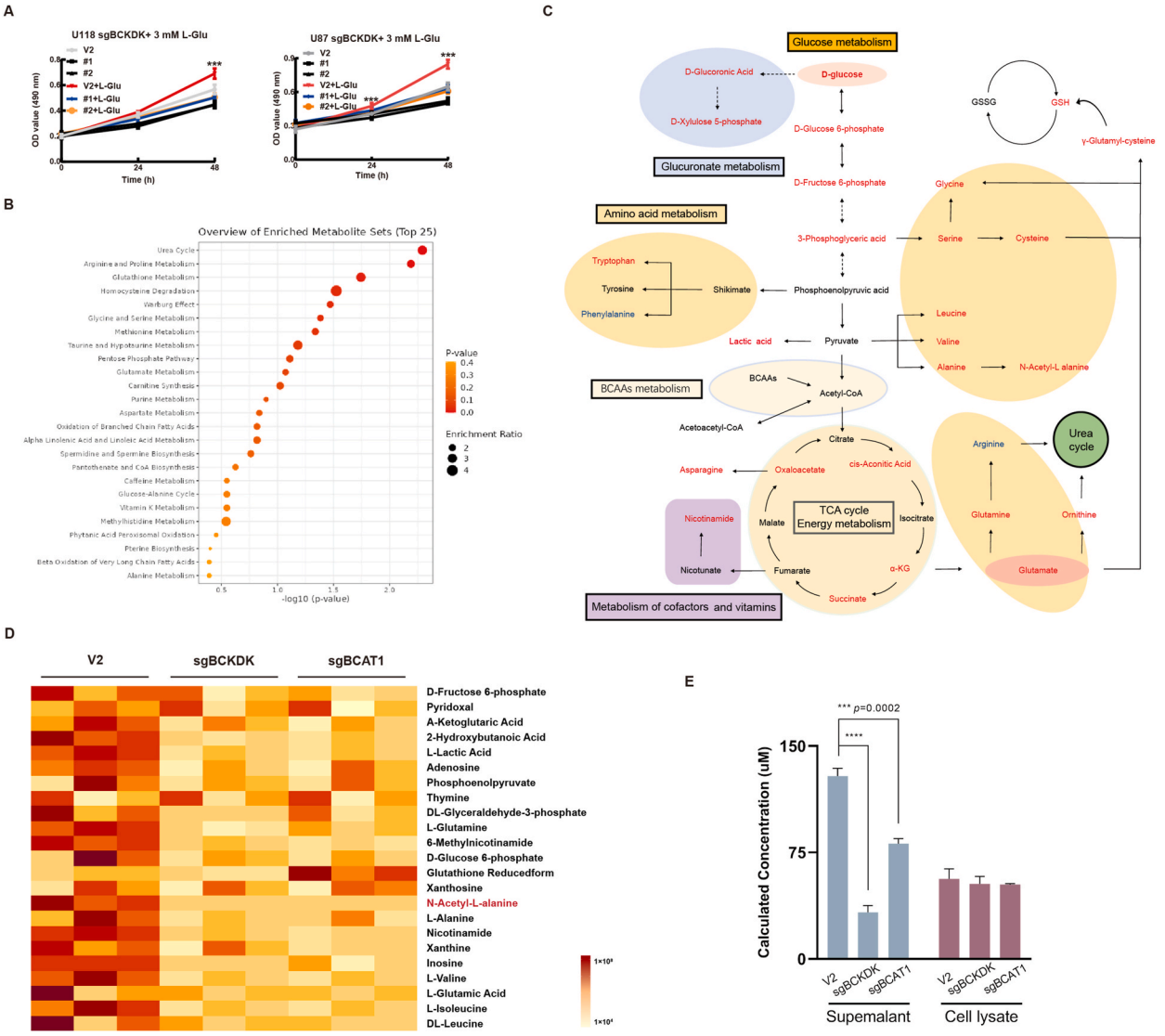

Fig. 5. BCKDK promotes metabolic reprogramming in gliomas and metabolite NAAL production A, Growth curves of control cells and BCKDK-silenced cells treated with Glu by MTT assay. Data are expressed as the mean ± SD of three replicates. B, Classification and enrichment map of the differential metabolite KEGG after silencing BCKDK and BCAT1. C, The metabolite signaling network of sgBCKDK and sgBCAT1 cells co-varying is presented, with red font indicating a decrease in the level of the metabolite, blue indicating an increase, and black font indicating no metabolite detected. D, Heatmap showing control versus sgBCKDK and sgBCAT1 differential metabolite content. E, Statistical plots of NAAL levels in NAAL standards, U118 sgBCKDK, sgBCAT1 cells and culture supernatants determined by UPLC/ESI-Q TRAP-MS-MS. . (For interpretation of the references to color in this figure legend, the reader is referred to the Web version of this article.)

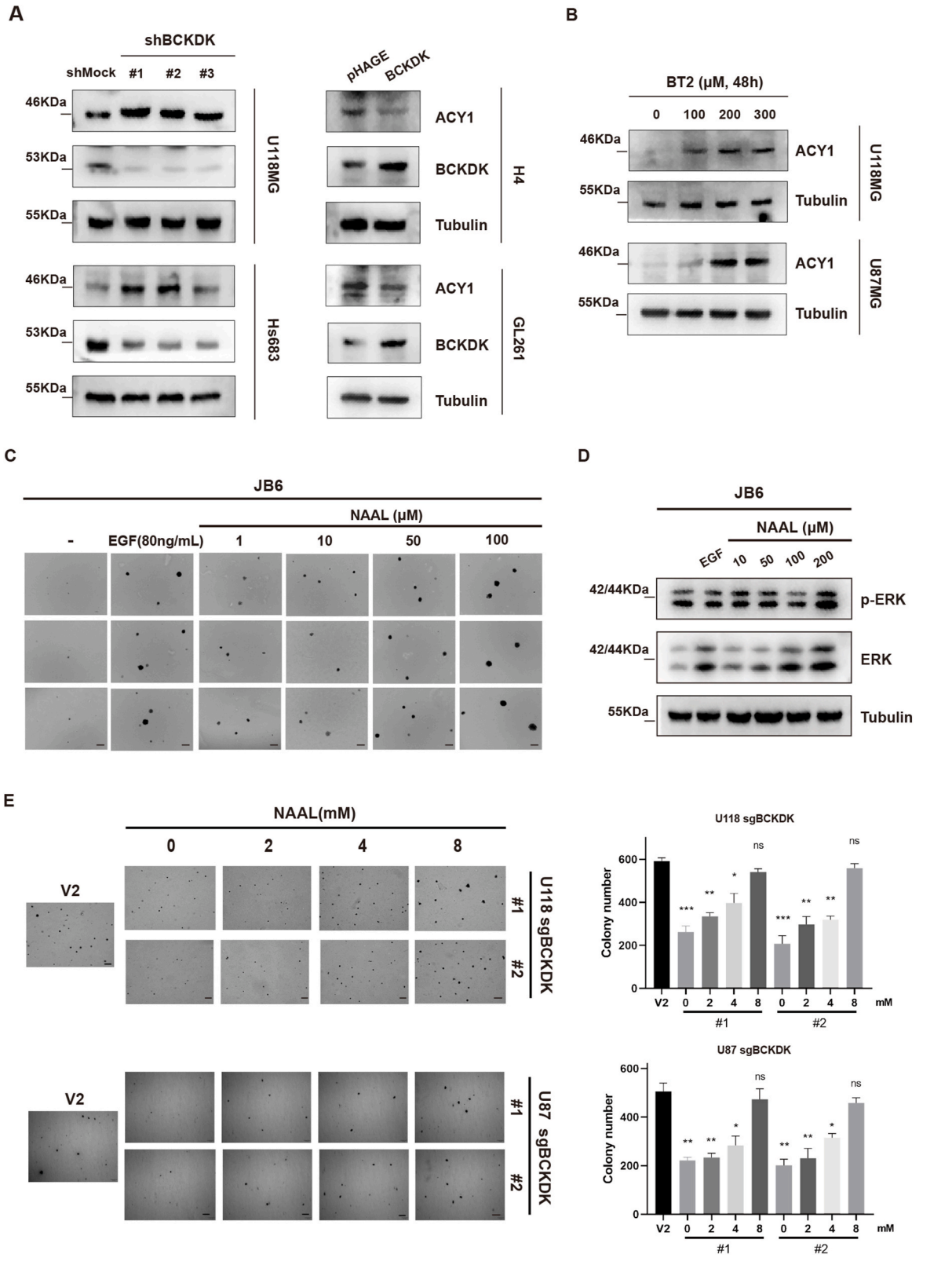

(caption on next page)

Fig. 6. BCKDK inhibit ACY1 expression and NAAL is an oncogenic metabolite A, WB detection of ACY1 expression in silenced (right) or overexpressed (left) BCKDK cell lines; B, WB detection of ACY1 expression in U118 and U87 cells after treatment with different concentrations of BT2 for 48 h. C, Soft agar assay of JB6 cells treated EGF (80 ng/ mL) or different concentrations NAAL. The data are presented as the mean ± SD of three replications. Scale bar: 400 μm. D, WB assay for *p*-ERK levels in EGF (80 ng/ mL) and NAAL-stimulated JB6 Cl41 cells for 48 h; E, Soft agar observation of JB6 cells in response to NAAL stimulation, EGF (80 ng/mL) stimulation was used as a positive control, and image acquisition was performed on day 21 post-stimulation (scale bar: 400 μm). The data are presented as the mean ± SD of three replications. (*$p < 0.05$, **$p < 0.01$, ***$p < 0.001$).

The $t_{1/2}$ of BCKDK-Y151F was significantly shorter than that of BCKDK-WT and BCKDK-Y151D by CHX chase experiments (Fig. 4B). In addition, it was found that the ubiquitination level of BCKDK-WT was significantly lower than that of BCKDK-Y151F (Fig. 4C), while the ubiquitination level difference between BCKDK-WT and BCKDK-Y151D was not significant (Fig. 4D). These results suggested that Fyn-mediated phosphorylation of BCKDK at Y151 protects it from ubiquitination degradation and enhances its stability. Next, MTT assay and colony formation assay showed that phosphorylation of BCKDK at the Y151 site promoted GBM cell growth (Fig. 4E–F), and transplanted GL261-Luc-BCKDK-Y151D tumors grew significantly faster than those with BCKDK-Y151F in the brains of C57BL/6 mice and mice with GL261-Luc-BCKDK-Y151F had longer survival (Fig. 4G and H). Taken together, Fyn phosphorylation of the Y151 site of BCKDK enhances its activity and stability, promotes glioma growth *in vitro* and *in vivo,* and also can be used as an observational marker for clinical evaluation of BCKDK activity in gliomas.

3.5. BCKDK promotes metabolic reprogramming in gliomas and metabolite NAAL production

BCKDK is not only involved in BCAA metabolism, but may also be involved in the regulation of glucose and lipid metabolism by phosphorylating PDC and ACL, so BCKDK could directly affect the level of metabolites and thus participate in tumor metabolic reprogramming. It was reported that high expression of BCAT1 increased the production of the pro-carcinogenic metabolite Glu (glutamate) and that inhibition of BCAT1 impaired Glu biosynthesis and redox homeostasis in GBM, which in turn inhibited tumor growth [33,34]. Our recent results demonstrate that BCKDK can phosphorylate and activate BCAT1 to promote GBM growth [21], we therefore speculated whether BCKDK could promote Glu synthesis and affect GBM cell growth. So we added 3 mM Glu to the medium to observe the effect of exogenous Glu on the growth of sgBCKDK cells, the results showed that exogenous Glu supplementation did not completely counteract the inhibitory effect of sgBCKDK on cell growth (Fig. 5A), suggesting that silencing of BCKDK may cause alterations in other metabolites, which may affect the growth of GBM. So, we compared the metabolite changes in intracellular metabolites of U118 V2, sgBCKDK, and sgBCAT1 by non-targeted metabolomics analysis. Fig. 5B showed that metabolite levels decreased in U118-sgBCKDK and sgBCAT1, and involved in a variety of metabolic pathways, including glucose metabolism, amino acid metabolism, glucuronidation, urea cycle and energy. And Fig. 5C listed some of these obvious differential metabolite signaling network maps. This suggestsed that BCKDK is not only involved in regulating BCAA metabolism, but can also affect multiple metabolic pathways in glioma cells.

Based on these results, we subsequently performed heatmap analysis of metabolites with significant and representative changes and found significantly reduced levels of BCAA, Glu, α-KG, GSH, L-alanine, glucose 6-phosphate, fructose 6-phosphate, and a number of nucleotides, which have also been reported to be strongly associated with tumour development. We screened for two metabolites that are currently not reported to be significantly reduced in association with tumors: 6-methylnicotinamide (6-MN) and N-acetyl-L-alanine (NAAL). And validation by exogenous addition in glioma cells revealed that 6-MN did not promote the proliferation of glioma cells U118 and U87, but NAAL did (Fig. S2A, B). Based on the above analyses, we will conduct further research on NAAL. Firstly, we measured the concentration of NAAL in the intracellular and culture supernatants of three cells, and the results showed that the level of NAAL in the cell culture supernatant of U118 V2 cells was significantly higher than that of U118 sgBCKDK or sgBCAT1, but there was no significant difference in intracellular content (Fig. 5E). These results suggested that NAAL could be secreted from the cells into the cell culture fluid, and that BCKDK influences the production and secretion of NAAL in the cells.

3.6. BCKDK inhibit ACY1 expression and NAAL is an oncogenic metabolite

Studies have shown that NAAL is a derivative of L-alanine, which can be produced either by direct acetylation of alanine by N-acetyltransferases (NAT) or by hydrolysis of N-acetylated proteins by hydrolases such as Aminoacetylase I (ACY1) [35]. Our results showed that the levels of ACY1 increased in BCKDK-knockdown cells and decreased in BCKDK-overexpressed cells (Fig. 6A). Moreover, the level of ACY1 increased in a dose-dependent manner after treatment with U118 and U87 cells with BCKDK inhibitor BT2 (Fig. 6B). These results indicated that BCKDK promotes NAAL production by inhibiting the expression of ACY1 in gliomas.

In order to reveal the role of NAAL production in tumor cell growth, we first observed the effect of NAAL on the transformed growth of the most common cell transformation model, mouse epidermal keratinocytes JB6 Cl41. The soft agar assay results showed that NAAL promoted JB6 Cl41 cell clone formation in a dose dependent manner, and the size of cell clones in the 100 μM NAAL group was similar to that of the positive EGF-stimulated group (Fig. 6C), suggesting that NAAL may be a oncogenic metabolite. Further studies revealed that NAAL could activate the ERK signaling pathway (Fig. 6D) and exogenous addition of NAAL could promote the growth of U118 sgBCKDK cells (Fig. S2A) and clone formation of U118 or U87-sgBCKDK cells (Fig. 6E). And NAAL also could increase the level of phosphorylated ERK in U87 cells (Fig. S2B). In summary, NAAL was an novel oncogenic metabolite that could activate ERK signaling pathway to promote cell transformation and glioma cell proliferation.

In conclusion, we identified the Fyn-BCKDK axis as a novel signaling pathway associated with GBM growth, and can further

promote tumor progression by affecting the levels of the metabolite NAAL. These findings suggest that *p*-BCKDK (Y151) and NAAL can serve as potential predictors of GBM progression and prognosis, providing new potential targets for targeted therapy of GBM.

4. Discussion

Some studies found that activated BCKDK played a key role in the occurrence and development of cancer [20,36]. BCKDK as a dark kinase needs to be further researched. Why does BCKDK show low expression or low activity in normal tissue cells and high expression and activation in tumor cells? In this study, we found that another protein kinase besides Src, Fyn, can phosphorylate and activate BCKDK, and the phosphorylation site is different from the known Y246 site, is Y151. Phosphorylation at Y151 increased the activity and stability of BCKDK and promoted tumor growth, as did phosphorylation at Y246. Our results showed that elevated BCKDK and *p*-BCKDK (Y151) expression levels were positively associated with GBM and negative prognosis in GBM patients, suggesting its potential role as a therapeutic target in glioma. Hence, it is necessary to conduct more basic experiments and expand glioma pathological specimens to further confirm the impact of BCKDK in glioma, thereby providing more reliable and comprehensive conclusions for clinical trials.

BCKDK as a dark kinase needs to be further researched. The activation mechanism of BCKDK is different in different cell background, especially in tumor cells. Activated BCKDK can modify different downstream substrates, which form a unique signal pathway and maintain the specific biological performance of tumor cells. In particular, the molecular mechanism of tumor metabolic reprogramming, how tumor driver genes directly regulate key metabolic enzymes. Moreover, BCKDK also serves as a bridge between BCAA metabolism, glucose metabolism and lipid metabolism, which is sufficient to demonstrate the profound significance of BCKDK as an emerging kinase target in cancer [18]. Therefore, exploring whether there are other downstream substrates of BCKDK also provides valuable options and strategies for better understanding the mechanism of tumor cell proliferation and targeted therapy. In addition, it has been shown that BCAT1 can maintain the low differentiation characteristics of GBM and contribute to immunosuppression of the tumor microenvironment, so whether BCKDK also plays an indispensable role in the tumor microenvironment, and whether it is able to participate in the tumor immunity and thus regulate the progression of the tumor cells is also a worthwhile direction of research.

Metabolic reprogramming, including aerobic glycolysis, lipid metabolism and BCAAs, is a marked feature of many solid tumors. The change of metabolism not only supply excess energy to fuel cancer cells growth and metastasis, but also produce lots of abnormal intermediates which can impact the genome stability, biosynthesis of macromolecules, and tumor microenvironment. The aberration of BCAAs catabolism and glutamate synthesis promotes the proliferation and aggression of malignant glioma [9,37]. Our study demonstrated that BCKDK was able to further activate the ERK signalling pathway and promote the proliferation of glioma cells by inhibiting the expression of ACY1 in order to increase the level of NAAL in glioma cells. In addition, NAAL is a small molecule compound that promotes the proliferation of glioma cells by activating the ERK signaling pathway, however, the target proteins it interacts with and the corresponding biological functions are not yet clear. On the other hand, this study demonstrated that NAAL can act as an oncogenic metabolite, but this conclusion still needs to be further tested and verified in the serum of normal subjects and tumor patients. Meanwhile, the development of a simple NAAL detection method is also very meaningful for the clinical detection and application of cancer.

Taken together, this study identified that BCKDK is highly expressed in GBM and promotes elevated levels of the related metabolite NAAL. Phosphorylation of the Y151 site of BCKDK by Fyn enhances its activity and stability and promotes glioma growth, suggesting the significant role of the Fyn-BCKDK axis in the growth of human GBM and providing new potential targets for targeted therapy of GBM.

5. Limitation

Our study demonstrated the important role of BCKDK expression and phosphorylation of the Y151 site in determining glioma development and prognosis, and we prepared an antibody to Y151. However, we need to test the specificity and sensitivity of this antibody in a larger number of clinical samples, which awaits further expansion of our study. On the other hand, we found that BCKDK was able to affect the levels of the oncogenic metabolite NAAL in gliomas, causing cell proliferation through activation of the ERK signalling pathway, but whether the activating effect on ERK is direct remains to be confirmed. Therefore, our next step should be to explore the target proteins of NAAL to understand the direct pathway of its biological function, which is necessary for us to better understand the biological effects of NAAL. Meanwhile, our study found that NAAL can promote glioma cell proliferation, so does it have a universal effect in all tumors? And further determination of the differences in the expression and content of BCKDK and NAAL in tumour patients and normal subjects is also fundamental to our better understanding of the relationship between BCKDK and NAAL.

Funding information

This study was supported by the National Natural Science Foundation of China (No. 81972762). The Independent innovation project of Huazhong University of Science and Technology (No. 2018KFYYXJJ084).

Informed consent

The clinical specimens were reviewed by the Medical Ethics Committee of Tongji Medical College, Huazhong University of Science and Technology, and unanimously believed that the design of the research protocol conformed to the principles of the Declaration of

Helsinki and fully respected the informed consent of the subjects and their families.

Animal studies

The experimental protocol complied with the Hubei Provincial Regulations on the Administration of Laboratory Animals and the Regulations of the Laboratory Animal Ethics Committee of HUST, and was approved by the Laboratory Animal Ethics Committee of Tongji Medical College of HUST with the approval number: [2021] IEC (A224), dated Mar 4, 2021.

Data availability statement

Data availability does not apply to this paper as no new data was created or analyzed for this study. Some of the results of the study, such as the results of the off-target metabolite screen, are listed (see Table 3).

Question: Has data associated with your study been deposited into a publicly available repository?

Answer: No, No data was used for the research described in the article.

CRediT authorship contribution statement

Ling Zou: Writing – original draft, Validation, Formal analysis, Data curation, Conceptualization. **Wei Wang:** Writing – original draft, Validation, Investigation, Formal analysis, Data curation, Conceptualization. **Wenda Huang:** Software, Formal analysis, Conceptualization. **Xiaofang Ni:** Formal analysis, Conceptualization. **Wensheng Li:** Validation, Data curation. **Yue Cheng:** Validation. **Qin Tian:** Conceptualization. **Lin Liu:** Supervision, Funding acquisition, Conceptualization. **Feng Zhu:** Visualization, Supervision, Funding acquisition, Conceptualization. **Qiuhong Duan:** Writing – review & editing, Visualization, Supervision, Project administration, Methodology, Investigation, Conceptualization.

Declaration of competing interest

The authors declare the following financial interests/personal relationships which may be considered as potential competing interests:Feng Zhu reports financial support was provided by National Natural Science Foundation of China. If there are other authors, they declare that they have no known competing financial interests or personal relationships that could have appeared to influence the work reported in this paper.

Acknowledgements

We would like to thank the other members of the Duan and Zhu Lab for their assistance and suggestions. We also thank Professor Dongsheng Guo (Tongji Hospital) for providing the tissue samples of glioma patients. We thank for the technical support by the Huazhong University of Science & Technology Analytical & Testing center,Medical sub-center. We thank Yizi Liu (Purdue, Wuhan, China) for providing analytical guidance related to the mass spectrometry results.

Abbreviations

ACY1	Aminoacetylase I
BCAA	Branched-Chain Amino Acid
BCKDC	Branched-chain α-keto acid dehydrogenase complex
BCKDHA	Branched-chain α-keto acid dehydrogenase
BCKDK	Branched-chain α-keto acid dehydrogenase kinase
BCKA	Branch-chain α-ketoacids
CHX	Cycloheximide
GBM	Glioblastoma
Glu	glutamate
IP	Immunoprecipitation
mOS	median overall survival
MTT	3-(4,5-dimethylthiazol-2-yl)-2,5-diphenyltetrazolium bromide
MS	Mass spectrometry
NAAL	N-acetyl-L-alanine
UPLC	Ultra Performance Liquid Chromatography

Appendix A. Supplementary data

Supplementary data related to this article can be found at https://doi.org/10.1016/j.heliyon.2024.e33663.

References

[1] H. Ohgaki, P. Kleihues, Population-based studies on incidence, survival rates, and genetic alterations in astrocytic and oligodendroglial gliomas, J. Neuropathol. Exp. Neurol. 64 (6) (2005) 479–489.
[2] D.N. Louis, et al., The 2016 World Health Organization classification of tumors of the central nervous system: a summary, Acta Neuropathol. 131 (6) (2016) 803–820.
[3] P.Y. Wen, D.A. Reardon, Neuro-oncology in 2015: progress in glioma diagnosis, classification and treatment, Nat. Rev. Neurol. 12 (2) (2016) 69–70.
[4] N.A. Bush, S.M. Chang, M.S. Berger, Current and future strategies for treatment of glioma, Neurosurg. Rev. 40 (1) (2017) 1–14.
[5] Q.T. Ostrom, et al., The epidemiology of glioma in adults: a "state of the science" review, Neuro Oncol. 16 (7) (2014) 896–913.
[6] F.E. Bleeker, R.J. Molenaar, S. Leenstra, Recent advances in the molecular understanding of glioblastoma, J. Neuro Oncol. 108 (1) (2012) 11–27.
[7] D. Hanahan, R.A. Weinberg, Hallmarks of cancer: the next generation, Cell 144 (5) (2011) 646–674.
[8] P.S. Ward, C.B. Thompson, Metabolic reprogramming: a cancer hallmark even warburg did not anticipate, Cancer Cell 21 (3) (2012) 297–308.
[9] M. Tonjes, et al., BCAT1 promotes cell proliferation through amino acid catabolism in gliomas carrying wild-type IDH1, Nat. Med. 19 (7) (2013) 901–908.
[10] L.S. Silva, et al., Branched-chain ketoacids secreted by glioblastoma cells via MCT1 modulate macrophage phenotype, EMBO Rep. 18 (12) (2017) 2172–2185.
[11] A. Hattori, et al., Cancer progression by reprogrammed BCAA metabolism in myeloid leukaemia, Nature 545 (7655) (2017) 500–504.
[12] Z. Gu, et al., Loss of EZH2 reprograms BCAA metabolism to drive leukemic transformation, Cancer Discov. 9 (9) (2019) 1228–1247.
[13] M.A. García-Espinosa, et al., Widespread neuronal expression of branched-chain aminotransferase in the CNS: implications for leucine/glutamate metabolism and for signaling by amino acids, J. Neurochem. 100 (6) (2007) 1458–1468.
[14] T.R. Hall, et al., Branched chain aminotransferase isoenzymes. Purification and characterization of the rat brain isoenzyme, J. Biol. Chem. 268 (5) (1993) 3092–3098.
[15] A.J. Sweatt, et al., Branched-chain amino acid catabolism: unique segregation of pathway enzymes in organ systems and peripheral nerves, Am. J. Physiol. Endocrinol. Metab. 286 (1) (2004) E64–E76.
[16] R.A. Harris, et al., Overview of the molecular and biochemical basis of branched-chain amino acid catabolism, J. Nutr. 135 (6 Suppl) (2005), 1527s-30s.
[17] A. Suryawan, et al., A molecular model of human branched-chain amino acid metabolism, Am. J. Clin. Nutr. 68 (1) (1998) 72–81.
[18] M.P. East, T. Laitinen, C.R.M. Asquith, BCKDK: an emerging kinase target for metabolic diseases and cancer, Nat. Rev. Drug Discov. 20 (7) (2021) 498.
[19] P. Xue, et al., BCKDK of BCAA catabolism cross-talking with the MAPK pathway promotes tumorigenesis of colorectal cancer, EBioMedicine 20 (2017) 50–60.
[20] Q. Tian, et al., Phosphorylation of BCKDK of BCAA catabolism at Y246 by Src promotes metastasis of colorectal cancer, Oncogene 39 (20) (2020) 3980–3996.
[21] W. Wang, et al., Cross-talk between BCKDK-mediated phosphorylation and STUB1-dependent ubiquitination degradation of BCAT1 promotes GBM progression, Cancer Lett. 591 (2024) 216849.
[22] S.L. Ibrahim, et al., Inhibition of branched-chain alpha-keto acid dehydrogenase kinase augments the sensitivity of ovarian and breast cancer cells to paclitaxel, Br. J. Cancer 128 (5) (2023) 896–906.
[23] C. Xu, et al., BCKDK regulates breast cancer cell adhesion and tumor metastasis by inhibiting TRIM21 ubiquitinate talin1, Cell Death Dis. 14 (7) (2023) 445.
[24] M. Xue, et al., Loss of BCAA catabolism enhances Rab1A-mTORC1 signaling activity and promotes tumor proliferation in NSCLC, Transl Oncol 34 (2023) 101696.
[25] M.E. Berginski, et al., The Dark Kinase Knowledgebase: an online compendium of knowledge and experimental results of understudied kinases, Nucleic Acids Res. 49 (D1) (2021) D529–d535.
[26] P.J. White, et al., The BCKDH kinase and phosphatase integrate BCAA and lipid metabolism via regulation of ATP-citrate lyase, Cell Metabol. 27 (6) (2018) 1281–1293 e7.
[27] L. Heinemann-Yerushalmi, et al., BCKDK regulates the TCA cycle through PDC in the absence of PDK family during embryonic development, Dev. Cell 56 (8) (2021) 1182–1194.e6.
[28] M. Zhai, et al., APN-mediated phosphorylation of BCKDK promotes hepatocellular carcinoma metastasis and proliferation via the ERK signaling pathway, Cell Death Dis. 11 (5) (2020) 396.
[29] A. Comba, et al., Fyn tyrosine kinase, a downstream target of receptor tyrosine kinases, modulates antiglioma immune responses, Neuro Oncol. 22 (6) (2020) 806–818.
[30] S. Guo, et al., NT5DC2 promotes tumorigenicity of glioma stem-like cells by upregulating fyn, Cancer Lett. 454 (2019) 98–107.
[31] S. Kant, et al., Perhexiline demonstrates FYN-mediated antitumor activity in glioblastoma, Mol. Cancer Therapeut. 19 (7) (2020) 1415–1422.
[32] R. Liu, et al., Tyrosine phosphorylation activates 6-phosphogluconate dehydrogenase and promotes tumor growth and radiation resistance, Nat. Commun. 10 (1) (2019) 991.
[33] S.K. McBrayer, et al., Transaminase inhibition by 2-hydroxyglutarate impairs glutamate biosynthesis and redox homeostasis in glioma, Cell 175 (1) (2018) 101–116.e25.
[34] B. Zhang, et al., Targeting BCAT1 combined with α-ketoglutarate triggers metabolic synthetic lethality in glioblastoma, Cancer Res. 82 (13) (2022) 2388–2402.
[35] J. Perrier, et al., Catabolism of intracellular N-terminal acetylated proteins: involvement of acylpeptide hydrolase and acylase, Biochimie 87 (8) (2005) 673–685.
[36] M. Zhai, et al., APN-mediated phosphorylation of BCKDK promotes hepatocellular carcinoma metastasis and proliferation via the ERK signaling pathway, Cell Death Dis. 11 (5) (2020) 396.
[37] E.H. Panosyan, et al., Clinical aggressiveness of malignant gliomas is linked to augmented metabolism of amino acids, J. Neuro Oncol. 128 (1) (2016) 57–66.